AFRL-RV-PS-
TP-2015-0001

AFRL-RV-PS-
TP-2015-0001

# MUTUAL NEUTRALIZATION OF ATOMIC RARE-GAS CATIONS (Ne+, Ar+, Kr+, Xe+) WITH ATOMIC HALIDE ANIONS (Cl−, Br−, I−)

**Nicholas S. Shuman, et al.**

**7 January 2015**

**Journal Article**




**AIR FORCE RESEARCH LABORATORY**
**Space Vehicles Directorate**
**3550 Aberdeen Ave SE**
**AIR FORCE MATERIEL COMMAND**
**KIRTLAND AIR FORCE BASE, NM 87117-5776**

# REPORT DOCUMENTATION PAGE

*Form Approved*
*OMB No. 0704-0188*



| **1. REPORT DATE** *(DD-MM-YYYY)* | **2. REPORT TYPE** | **3. DATES COVERED** *(From - To)* |
|---|---|---|
| 07-01-2015 | Journal Article | 01 Aug 2013 – 06 Nov 2013 |

**4. TITLE AND SUBTITLE**
Mutual neutralization of atomic rare-gas cations (Ne+, Ar+, Kr+, Xe+) with atomic halide anions (Cl−, Br−, I−)

**5a. CONTRACT NUMBER**

**5b. GRANT NUMBER**

**5c. PROGRAM ELEMENT NUMBER**
61102F

**6. AUTHOR(S)**
Nicholas S. Shuman, Thomas M. Miller, Rainer Johnsen[1], and Albert A. Viggiano

**5d. PROJECT NUMBER**
2303

**5e. TASK NUMBER**
PPM00004294

**5f. WORK UNIT NUMBER**
EF002012

**7. PERFORMING ORGANIZATION NAME(S) AND ADDRESS(ES)**
Air Force Research Laboratory
Space Vehicles Directorate
3550 Aberdeen Avenue SE
Kirtland AFB, NM 87117-5776

[1]Department of Physics and Astronomy
University of Pittsburgh
4200 Fifth Avenue
Pittsburgh, PA 15260

**8. PERFORMING ORGANIZATION REPORT NUMBER**
AFRL-RV-PS-TP-2015-0001

**9. SPONSORING / MONITORING AGENCY NAME(S) AND ADDRESS(ES)**

**10. SPONSOR/MONITOR'S ACRONYM(S)**
AFRL/RVBXT

**11. SPONSOR/MONITOR'S REPORT NUMBER(S)**

**12. DISTRIBUTION / AVAILABILITY STATEMENT**
Approved for public release; distribution is unlimited. (377ABW-2013-0928 dtd 23 Oct 2013)

**13. SUPPLEMENTARY NOTES**
Accepted for publication in The Journal of Chemical Physics: 12 November 2014. Government Purpose Rights.

**14. ABSTRACT**
We report thermal rate coefficients for 12 reactions of rare gas cations ($Ne^+$, $Ar^+$, $Kr^+$, $Xe^+$) with halide anions ($Cl^-$, $Br^-$, $I^-$), comprising both mutual neutralization (MN) and transfer ionization. No rate coefficients have been previously reported for these reactions; however, the development of the Variable Electron and Neutral Density Attachment Mass Spectrometry technique makes it possible to measure the difference of the rate coefficients for pairs of parallel reactions in a Flowing Afterglow-Langmuir Probe apparatus. Measurements of 18 such combinations of competing reaction pairs yield an over-determined data set from which a consistent set of rate coefficients of the 12 MN reactions can be deduced. Unlike rate coefficients of MN reactions involving at least one polyatomic ion, which vary by at most a factor of ~3, those of the atom-atom reactions vary by at least a factor 60 depending on the species. It is found that the rate coefficients involving light rare-gas ions are larger than those for the heavier rare-gas ions, but the opposite trend is observed in the progression from $Cl^-$ to $I^-$. The largest rate coefficient is $6.5 \times 10^{-8}$ $cm^3$ $s^{-1}$ for $Ne^+$ with $I^-$. Rate coefficients for $Ar^+$, $Kr^+$, and $Xe^+$ reacting with $Br2^-$ are also reported.

**15. SUBJECT TERMS**
Physical Chemistry, Atomic and Molecular Chemistry, Atom reactions, ion ion reactions, plasma flows, diffusion, data analysis

| **16. SECURITY CLASSIFICATION OF:** | | | **17. LIMITATION OF ABSTRACT** | **18. NUMBER OF PAGES** | **19a. NAME OF RESPONSIBLE PERSON** |
|---|---|---|---|---|---|
| **a. REPORT** | **b. ABSTRACT** | **c. THIS PAGE** | | | Dr. Albert Viggiano |
| Unclassified | Unclassified | Unclassified | Unlimited | 12 | **19b. TELEPHONE NUMBER** *(include area code)* |

# Mutual neutralization of atomic rare-gas cations ($Ne^+$, $Ar^+$, $Kr^+$, $Xe^+$) with atomic halide anions ($Cl^-$, $Br^-$, $I^-$)

Nicholas S. Shuman,[1] Thomas M. Miller,[1] Rainer Johnsen,[2] and Albert A. Viggiano[1,a)]
[1]*Air Force Research Laboratory, Space Vehicles Directorate, Kirtland Air Force Base, New Mexico 87117, USA*
[2]*Department of Physics and Astronomy, University of Pittsburgh, Pittsburgh, Pennsylvania 15260, USA*

(Received 6 November 2013; accepted 23 December 2013; published online 23 January 2014)

We report thermal rate coefficients for 12 reactions of rare gas cations ($Ne^+$, $Ar^+$, $Kr^+$, $Xe^+$) with halide anions ($Cl^-$, $Br^-$, $I^-$), comprising both mutual neutralization (MN) and transfer ionization. No rate coefficients have been previously reported for these reactions; however, the development of the Variable Electron and Neutral Density Attachment Mass Spectrometry technique makes it possible to measure the difference of the rate coefficients for pairs of parallel reactions in a Flowing Afterglow-Langmuir Probe apparatus. Measurements of 18 such combinations of competing reaction pairs yield an over-determined data set from which a consistent set of rate coefficients of the 12 MN reactions can be deduced. Unlike rate coefficients of MN reactions involving at least one polyatomic ion, which vary by at most a factor of ~3, those of the atom-atom reactions vary by at least a factor 60 depending on the species. It is found that the rate coefficients involving light rare-gas ions are larger than those for the heavier rare-gas ions, but the opposite trend is observed in the progression from $Cl^-$ to $I^-$. The largest rate coefficient is $6.5 \times 10^{-8}$ $cm^3$ $s^{-1}$ for $Ne^+$ with $I^-$. Rate coefficients for $Ar^+$, $Kr^+$, and $Xe^+$ reacting with $Br_2^-$ are also reported. © *2014 AIP Publishing LLC*. [http://dx.doi.org/10.1063/1.4862151]

## INTRODUCTION

The mutual destruction of positive ions and negative ions in ion-ion plasmas can occur by several mechanisms. Termolecular ion-ion recombination, in which energy is transferred to ambient gas atoms M,

$$A^+ + B^- + M \rightarrow A + B + M, \quad (1a)$$

$$\rightarrow AB + M \quad (1b)$$

has been treated theoretically in great detail by classical mechanics (see, e.g., Bates or Flannery).[1,2] In that case, the chemical nature of the recombining ions enters only weakly through their masses and ion-atom interaction potentials. In contrast, binary mutual neutralization (MN),

$$A^+ + B^- \rightarrow A + B \quad (2)$$

depends sensitively on the internal and electronic states of the interacting species. When both ions are atomic, MN must occur at intersections of the initial ionic potential curve and those describing the interaction between the atoms in their final states, as in "accidentally resonant" charge transfer of ions and atoms. Unlike reactions involving a polyatomic species, which will have a broad manifold of possible product electronic and vibrational states, an atom-atom system will have a sparse density of possible product electronic states. The rate coefficients for MN then depend critically on the chemical species involved and are not easily predictable by simple arguments.

With the exception of the $H^+ + H^-$ system, for which cross-sections have been determined by experiment[3] and calculation,[4] and a handful of other systems, experimental data on binary atomic MN reactions are rather sparse. Rate coefficients of atomic rare gas cations with halide anions ($Rg^+ + X^-$) reactions have been measured in high-pressure afterglows[5] but the extrapolation to low pressures is highly uncertain. There are quite a few theoretical estimates based on the Landau-Zener model,[6,7] and upper limits on four binary $Rg^+ + X^-$ MN rate coefficients have been determined experimentally in a flowing afterglow.[8] Accurate theoretical treatments are inherently difficult because curve crossings involving excited state species at large internuclear distance can contribute. Approximate scaling formulas[9,10] are useful to obtain rough estimates, but they rely on simplifying assumptions that may not be justified in all cases. The Double Electrostatic Storage Ring Ion Experiment will soon be brought online[11] and is expected to yield important new data on mutual neutralization; much like the advent of magnetic storage rings in the 1990s greatly advanced the study of dissociative recombination.

Recently, we have used the variable electron and neutral density attachment mass spectrometry (VENDAMS) technique[12] to study a wide variety of MN processes.[9] These include the first complete product distributions[13] and evidence that electrons catalyze the process.[14,15] The measurements rely on the difference in rate coefficients of, typically, $Ar^+$ with the anion of interest to that of $Ar^+$ with an atomic halide anion, the latter of which have been assumed to proceed at a negligible rate.[8,9] In this paper, using a slightly modified VENDAMS method, we describe the results of a series of

a)Author to whom corresponding should be addressed. Electronic mail: afrl.rvborgmailbox@kirtland.af.mil

 

measurements on binary mutual neutralization reactions of atomic rare gas cations with atomic halide anions.

Direct measurement of either cation or anion absolute densities under typical conditions in a flowing afterglow-Langmuir probe (FALP) apparatus using the standard "orbital-motion" theory is problematic due to collisions between ions and neutral species trapping ions near the probe and thereby artificially increasing the probe's target area.[16] Additionally, measurement of any MN rate coefficients smaller than $\sim 10^{-8}$ cm$^3$ s$^{-1}$ is difficult in traditional FALP measurements due to the competing rate of ambipolar diffusive loss. However, measurement of the relative concentration of either anions or cations in FALP mass spectra is routine and robust. By creating conditions with a single dominant cation and two or more anionic species, the change in the relative abundance of the anions as a function of the initial plasma density, with which the initial cation density scales, indicates the difference in the rate coefficients of the competing neutralization reactions. Importantly, only electron densities need to be measured absolutely, with all ion density measurements being relative. Similar experiments can be conducted by creating conditions with a single dominant anion and multiple cations. By making difference measurements of many combinations of both anions ($Cl^-$, $Br^-$, $I^-$) and cations ($Ne^+$, $Ar^+$, $Kr^+$, $Xe^+$), a ladder of reactivity for the series of reactions $Rg^+ + X^-$ is established. Because the same reactions are probed via monitoring either competing cations or competing anions, redundancy results in the ladder being over-determined, with internal consistency giving increased confidence in the resulting values. Third-body contributions due to neutral atoms are negligible at the experimental gas densities (on the order of $3 \times 10^{16}$ cm$^3$ s$^{-1}$ of He), as shown in a recent systematic study of a possible enhancement of MN rates.[17] Similarly, both the densities of ions (on the order of $10^9$—$10^{10}$ cm$^3$ s$^{-1}$) and electrons are too small to affect the rate coefficients.

In some of the reactions, the halogen product is formed in excited states with sufficient energy to autoionize to form $X^+ + e^-$,

$$Rg^+ + X^- \rightarrow Rg + X^*, \tag{3a}$$

$$\rightarrow Rg + X^+ + e^-. \tag{3b}$$

This process (3b) has not been reported previously for cation-anion neutralization, but is similar to transfer ionization (TI) observed in other classes of charge transfer. Results for TI of $Ar^+$ to $Br^-$ and $I^-$ are reported in Ref. 18. The rate coefficients reported here are for the sum of MN and TI, i.e., reactions (2), (3a), and (3b) although TI is endoergic and cannot occur in about half of the reported systems.

## EXPERIMENTAL

The measurements were made using the Air Force Research Laboratory's FALP apparatus using the VENDAMS technique, both of which have been described in detail previously.[12,19] At the upstream end of the 1 m long FALP, a helium (99.999%, Matheson) flow of 10–20 std. L min$^{-1}$ is ionized by a microwave discharge yielding $He^+$, $He_2^+$, $He^*$, and $e^-$. An Ar (99.999%, Matheson) flow of ~0.3 std. L min$^{-1}$ is added ~10 cm downstream converting $He_2^+$ and $He^*$ to $Ar^+$, yielding a plasma in which over 95% of the cations are $Ar^+$ with the remainder being $He^+$ and small levels of water and air ion impurities. By replacing the Ar with Kr or Xe, a similarly pure $Kr^+$ or $Xe^+$ plasma can be made. The reaction of $He^*$ with Ne to yield $Ne^+$ is endothermic, precluding production of a $Ne^+$ dominated plasma in the same manner. Alternatively, two rare gases instead of one may be added downstream, each through a separate mass flow meter but mixing prior to entering the flow tube through a single inlet, to yield a mixture of $Rg^+$ cations. Experiments were conducted in $Ar^+/Ne^+$, $Ar^+/Xe^+$, and $Ar^+/Kr^+$ plasmas with typically >80% $Ar^+$, 15% $Ne^+/Xe^+/Kr^+$, and <5% other cations. Typical FALP studies are conducted at ~1 Torr at 300 K; this study was conducted at higher pressure (1.5–2 Torr) in order to convert a larger fraction of $He^+$ into $He_2^+$, which then converts rapidly to $Rg^+$, thereby reducing the fraction of $He^+$ in the plasma.

Either one or two neutral attaching gases ($CCl_4$ (Sigma Aldrich) to yield $Cl^-$, $CF_2Br_2$ (Sigma Aldrich) to yield $Br^-$, or $C_2F_3I$ (SynQuest Labs) to yield $I^-$)[20,21] may be added to the afterglow through a glass inlet comprising 6 fingers evenly spaced on a 1 cm radius located 44 cm before the end of the flow tube. These reagents are prepared as dilute (0.5%–1.0%) mixtures in helium and added using mass flow meters. The liquid reagents, $CCl_4$ and $CF_2Br_2$, are purified via freeze-pump-thaw cycles prior to mixture preparation.

The absolute electron density along the center axis of the flow tube may be measured using a cylindrical Langmuir probe. The probe is movable from 15 cm before to 35 cm after the neutral inlet; however, with the exception of diffusion measurements, all electron density measurements here are made 1 cm upstream of the neutral reactant inlet, and reflect the initial electron density $[e]_0$ upon introduction of reactant species. $[e]_0$ may be varied over several orders of magnitude (in the present case from $\sim 10^8$ cm$^{-3}$ to $\sim 2 \times 10^{10}$ cm$^{-3}$) primarily by translating the microwave discharge cavity farther from or closer to the reactant inlet. Importantly, and in contrast to prior FALP studies of MN,[8] the Langmuir probe is used here only to measure electron, and not ion, densities. Prior to the introduction of any electron attaching species, the total cation concentration is assumed to be equal to the electron concentration (i.e., the plasma is neutral), and $[e]_0$ is taken as also a measurement of the plasma density. The center axis of the flow at the downstream end of the flow tube is sampled through a 0.3 mm diameter aperture in a truncated nosecone leading to a lens stack and quadrupole mass spectrometer. Ion velocity and ambipolar diffusion are measured using standard methods. Diffusion after conditions evolve into an ion/ion plasma is assumed to occur with a rate coefficient one half that measured in the cation/$e^-$ plasma.[22] Mass discrimination is not particularly important to the current experiments, but is measured where needed by methods previously described.[23]

Measurements were made for each pair of $Cl^-$, $Br^-$, and $I^-$ in each of the plasmas dominated by either $Ar^+$, $Kr^+$, or $Xe^+$. Experiments were attempted using 0.5% $F_2$ in He as

a source of $F^-$; however, significant chemistry appeared to occur between $F_2$ and the other neutral precursors in the inlet lines, resulting in unknown neutral concentrations entering the flow tube and precluding an accurate analysis of the data. Measurements were also made in $Ar^+/Xe^+$, $Ar^+/Kr^+$, and $Ar^+/Ne^+$ with each of the anions $Cl^-$, $Br^-$, and $I^-$. These experiments were not attempted with $F^-$, as $F_2$ attaches electrons inefficiently preventing the quick depletion of electron density with a low concentration of added neutral; this is an issue as the sampling efficiency and mass discrimination of the detection system changes significantly between a plasma with considerable concentrations of electrons and one without. The former would occur at high $[e]_0$ and the latter at low $[e]_0$. Nascent ratios of $Ar^+$:$Rg^+$ as a function of $[e]_0$ were measured without any attaching gas added. For both the $Ar^+/Xe^+$ and $Ar^+/Kr^+$ plasmas, this ratio was independent of $[e]_0$. The ratio in the $Ar^+/Ne^+$ showed structure with $[e]_0$ as discussed below.

## DATA AND ANALYSIS

The primary data in VENDAMS are relative ion concentrations measured after a fixed reaction time, typically 7.1 ms, as a function of $[e]_0$, as measured using the Langmuir probe just before the neutral inlet. The present measurements were performed one of two ways, either monitoring the concentrations of two cationic species in the presence of a single dominant anion, or the inverse, monitoring the concentrations of two anionic species in the presence of a single dominant cation.

For the former technique, two noble gases (e.g., Ar and Kr) are added to an upstream inlet to create an $Ar^+/Kr^+/e^-$ plasma as described above. Downstream, a single gas that rapidly attaches electrons is added in known concentration through the neutral inlet using a mass flow meter to convert all electrons into halide anions within a few cm; the complete electron depletion is confirmed using the Langmuir probe. $CCl_4$, $CF_2Br_2$, and $C_2F_3I$ were used to make $Cl^-$, $Br^-$, and $I^-$, respectively.[20,21] The neutral concentration is kept sufficiently low (typically $\sim 3 \times 10^{10}$ cm$^{-3}$) that reaction with $Rg^+$ occurs to only a small extent, and the cationic species in the plasma remain predominantly $Rg^+$. Representative data for $Ar^+/Kr^+$ reacting with $I^-$ are shown in Fig. 1. As the plasma density increases, the absolute concentration of $I^-$ formed via attachment increases and the abundance of $Ar^+$ decreases relative to that of $Kr^+$, reflecting a larger rate of reaction between $Ar^+$ and $I^-$ than between $Kr^+$ and $I^-$. In the particular case of the $Ar^+/Ne^+$ plasma, the nascent fraction of $Ne^+$ in the plasma varied with $[e]_0$ (Fig. 2). This background variation was incorporated into the modeling described below, increasing the uncertainty in the derived values.

The analogous anion measurements involve instead a plasma dominated by a single cation, either $Ar^+$, $Xe^+$, or $Kr^+$ as described above. Two attaching gases are added in known concentrations through separate mass flow meters, but through the same neutral inlet, yielding two atomic halide anions. The relative concentrations of the anions are monitored as a function of $[e]_0$, yielding information on the reactions of those anions with the dominant cation. Representative data

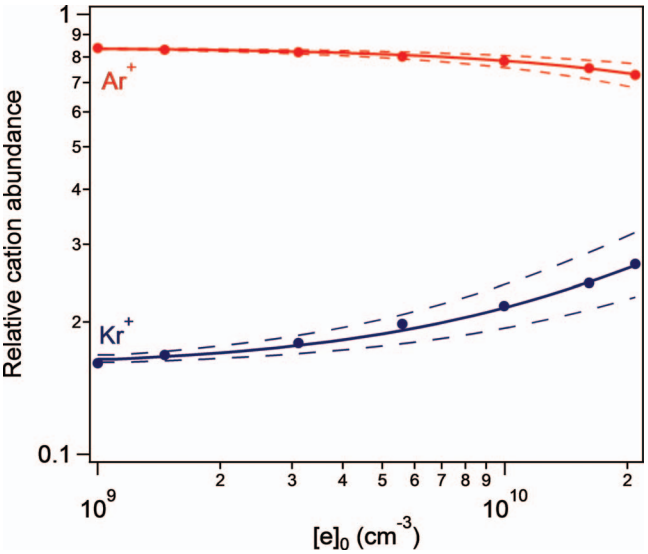


FIG. 1. Relative cation abundances as a function of initial electron density 7.1-ms after addition of $6.5 \times 10^{10}$ cm$^{-3}$ $C_2F_3I$ to an $Ar^+/Kr^+/e$ plasma at 300 K. Solid lines are best fit models; dashed lines are representative fits at the reported uncertainty limits.

from the addition of $CCl_4$ and $CF_2Br_2$ to an $Ar^+/e^-$ plasma is shown in Fig. 3. The $Br_2^-$ is due to a 7% branching in the electron attachment to $CF_2Br_2$;[20] however, the presence of the minor competing ion does not add significant difficulty to the analysis, and in fact adds ancillary information on the reaction of $Br_2^-$ with the $Rg^+$ species. Interpretation of the data here is similar to the cation case, indicating that $Br^-$ and $Cl^-$ react with $Ar^+$ at similar rates, with $Br^-$ being slightly faster, and $Br_2^-$ reacting significantly more rapidly with $Ar^+$.

While there is no simple analytic form to extract rate coefficients from the data, information on the rate coefficients

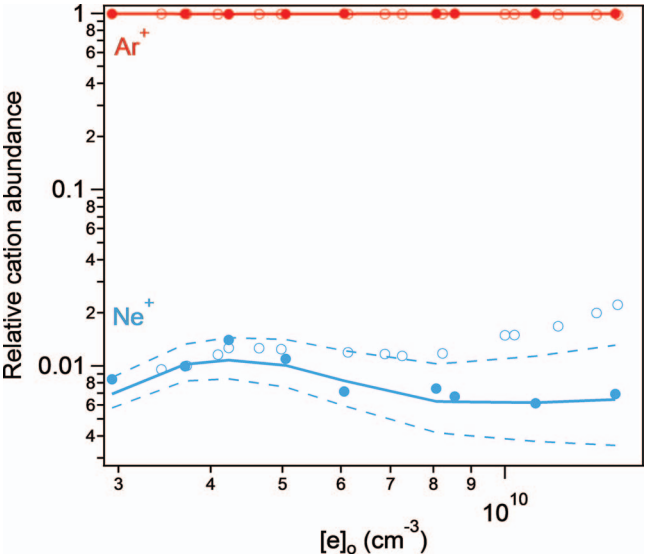


FIG. 2. Relative cation abundances as a function of initial electron density 7.1 ms after addition of $3.5 \times 10^{10}$ cm$^{-3}$ $C_2F_3I$ to an $Ar^+/Ne^+/e$ plasma at 300 K (solid points) and under the same conditions without addition of $C_2F_3I$ (open points). Solid lines are best fit models accounting for the nascent distribution of $Ar^+$:$Ne^+$; dashed lines are representative fits at the reported uncertainty limits.

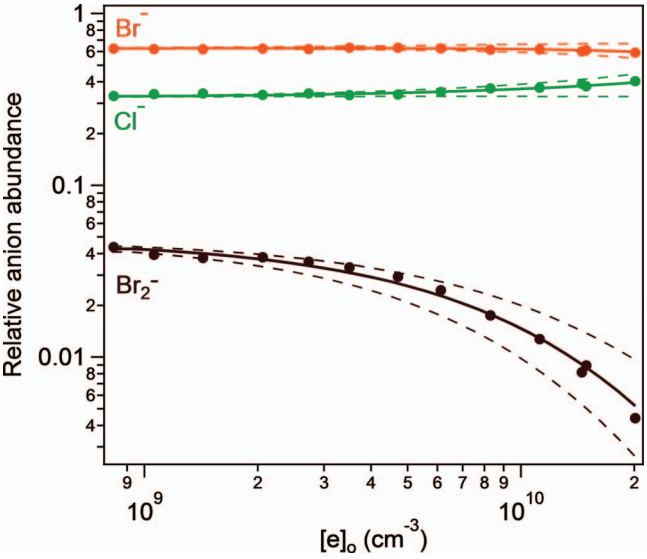


FIG. 3. Relative anion abundances as a function of initial electron density 7.1 ms after addition of $9.3 \times 10^9$ cm$^{-3}$ $CCl_4$ and $2.2 \times 10^{10}$ cm$^{-3}$ $CF_2Br_2$ to an $Ar^+$/e plasma at 300 K. Solid lines are best fit models; dashed lines are representative fits at the reported uncertainty limits.

of the competing reactions may be derived by numerically solving the rate equations describing the chemistry occurring in the flow tube from the known initial conditions throughout the known reaction time. As described in detail in Ref. 12, the full parameter space defined by uncertainties in rate coefficients, neutral concentrations, and diffusion coefficients is sampled through a Monte Carlo method, with calculated relative ion abundances compared to the measured data through a weighted least squares fit. While the complete chemistry is modeled, the data are almost exclusively sensitive to difference of the rate coefficients (comprising both MN and TI product channels) for the two competing reactions and the measured diffusion rate. The latter affects the total concentration of the species and therefore the rate of disappearance. It should be noted that all ions were treated as diffusing at the same rate. It is unclear if this assumption is justified; however, that the results of these measurements, which involve different pairs of ions yielding information on the same reaction rate constants, were self-consistent suggests that differential diffusion rates between the ions are small.

The data from each individual experiment here constrain the difference in the competing rate coefficients, as opposed to their absolute values. These results are compiled in Tables I and II. Because there is overlap in the reactions studied between experiments, these differences form a ladder connecting the set of $Rg^+/X^-$ rate coefficients. Because of the redundancy in the measurements between the two techniques (monitoring either anions or cations), the interconnected set is over-determined (Fig. 4(b)). That the over-determined set is self-consistent supports the validity of the measurements.

If any one of the rate coefficients in the ladder is known, then all the values can be put on an absolute scale. No two-body rate coefficients for $Rg^+/X^-$ systems have been reported in the literature; however, Church and Smith report upper limits of 0.2–1.0 $\times$ $10^{-8}$ cm$^3$ s$^{-1}$ for reactions of $F^-$ with $Ar^+$, $Kr^+$, and $Xe^+$, and an upper limit of $5 \times 10^{-9}$ cm$^3$ s$^{-1}$

TABLE I. Measured differences in the rate coefficients of $Ar^+ + X^-$ and $Rg^+ + X^-$.

| $X^-$ | $Rg^+$ | $k_{Ar^+ + X^-} - k_{Rg^+ + X^-}$ ($10^{-8}$ cm$^3$ s$^{-1}$) |
|---|---|---|
| $Cl^-$ | $Ne^+$ | $-2.6 \pm 1.1$ |
| | $Kr^+$ | $0.3\pm^{0.3}_{0.1}$ |
| | $Xe^+$ | $0.4\pm^{0.5}_{0.2}$ |
| $Br^-$ | $Ne^+$ | $-2.8 \pm 1.2$ |
| | $Kr^+$ | $0.5\pm^{0.4}_{0.2}$ |
| | $Xe^+$ | $0.5\pm^{0.4}_{0.3}$ |
| $I^-$ | $Ne^+$ | $-4.5 \pm 1.4$ |
| | $Kr^+$ | $1.2 \pm 0.2$ |
| | $Xe^+$ | $2.0\pm^{0.8}_{0.4}$ |

for $Xe^+ + Cl^-$, the latter of which appears in our data set providing a constraint for the present results.[8] Further, our ladder limits the rate coefficients for several of the reactions ($Kr^+ + Cl^-$, $Kr^+ + Br^-$, and all three $Xe^+$ reactions) to be the same value within about $2 \times 10^{-9}$ cm$^3$ s$^{-1}$, the sensitivity of the experiment. While it is possible that all of these reactions occur with similar rate coefficients close to the reported upper limit for $Xe^+ + Cl^-$, it appears more likely that all the reactions simply occur with a rate coefficient below the detection limit of the experiment. If we assume that any one of these five reactions occurs with a rate coefficient below $\sim 10^{-9}$ cm$^3$ s$^{-1}$, then this becomes an effective anchor for all the measured rate coefficients as it is much less than the experimental uncertainty. Therefore, in addition to the 18 analyses of the individual data sets yielding the difference measurements reported in Tables I and II, we have also analyzed 15 data sets (excluding those involving $Ne^+$, which lack redundancy) in concert with the constraint that $Xe^+ + Cl^-$ proceeds with $k \leq 10^{-9}$ cm$^3$ s$^{-1}$. The derived rate coefficients are shown in Fig. 4(a) and listed in Table III. The set of measurements was self-consistent, as demonstrated in Fig. 4(b) comparing the individual difference measurements to the derived rate coefficients; an inconsistent data set plotted in this manner would show some of the termini of the ball and chains outside of the shaded uncertainties for the derived absolute rate coefficients. It is worth noting that the $Ne^+$ rate coefficients are each

TABLE II. Measured differences in the rate coefficients of the indicated $Rg^+ + X^-$ and $Rg^+ + Y^-$ reactions.

| | | $k_{Rg^+ + X^-} - k_{Rg^+ + Y^-}$ ($10^{-8}$ cm$^3$ s$^{-1}$) | | |
|---|---|---|---|---|
| | | $X^-$ | | |
| $Rg^+$ | $Y^-$ | $Br^-$ | $I^-$ | $Br_2^-$ |
| $Ar^+$ | $Cl^-$ | $0.4\pm^{0.2}_{0.6}$ | $1.3\pm^{0.9}_{0.3}$ | $3.4 \pm 1.0$ |
| | $Br^-$ | ... | $1.1\pm^{0.4}_{0.3}$ | $3.2 \pm 0.9$ |
| | I- | ... | ... | $1.7 \pm 0.6$ |
| $Kr^+$ | $Cl^-$ | $-0.1 \pm 0.4$ | $0.8\pm^{0.6}_{0.3}$ | $3.3 \pm 0.8$ |
| | $Br^-$ | ... | $0.9\pm^{0.6}_{0.3}$ | $3.2 \pm 0.8$ |
| | I- | ... | ... | $2.3 \pm 0.8$ |
| $Xe^+$ | $Cl^-$ | $0.2\pm^{0.3}_{0.2}$ | $0.1 \pm 0.2$ | $4.9 \pm 1.6$ |
| | $Br^-$ | ... | $0.2\pm^{0.2}_{0.1}$ | $4.0 \pm 1.3$ |
| | I- | ... | ... | $3.0 \pm 1.6$ |

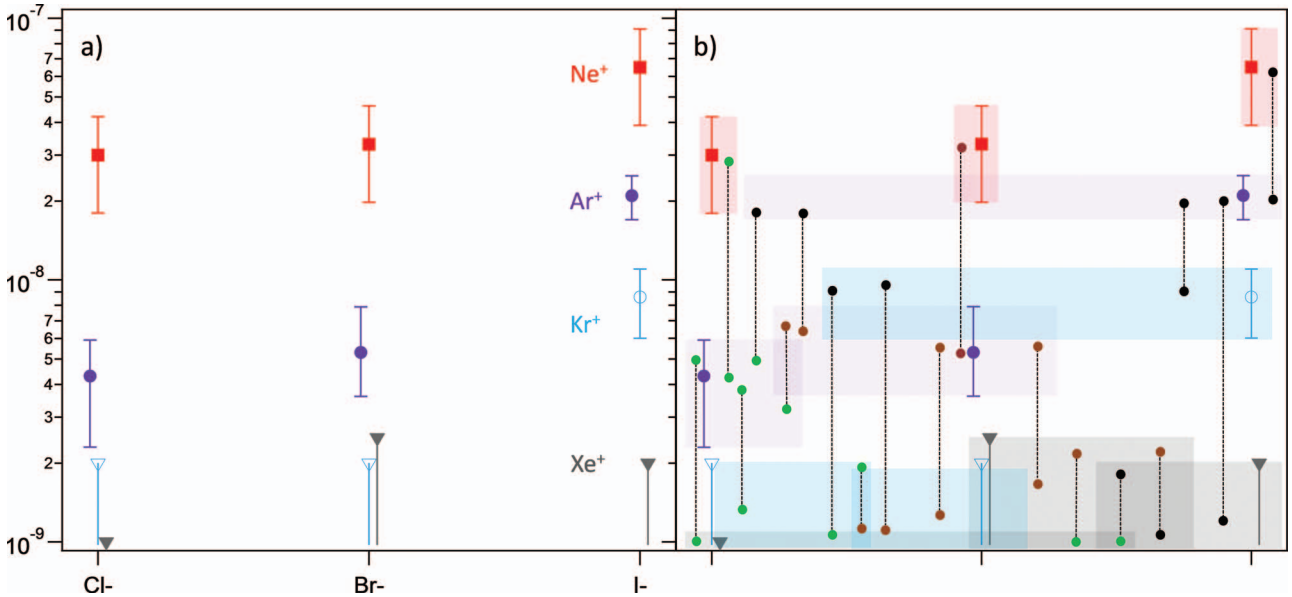


FIG. 4. (a) Derived rate coefficients for reactions of the indicated $Rg^+ + X^-$ at 300 K. Triangles indicate upper limits. (b) Representation of the over-determined ladder of measured differences in the $Rg^+ + X^-$ rate coefficients (see text). The derived rate coefficients are shown as in (a), and are overlayed with the measured differences (ball and chains) between the rate coefficients of the indicated reactions. Color of the balls indicates the relevant anion (green = $Cl^-$; brown = $Br^-$; black = $I^-$), while the shaded regions at each terminus indicate the cation (red = $Ne^+$; purple = $Ar^+$; blue = $Kr^+$; grey = $Xe^+$). The extents of the chains are the measured differences (typical uncertainty is 20%, not shown). Vertical extents of the shaded areas are at the uncertainty limits for each best-fit rate coefficient; horizontal extents of the shaded areas are for convenience of presentation only.

determined by a single measurement, the difference between the $Ne^+$ and $Ar^+$ rate coefficients for each anion, while all other reported values benefit from redundant measurements.

## DISCUSSION

This experimental study has produced a set of 12 rate coefficients for thermal reactions of rare-gas cations with atomic halide anions at room temperature, comprising both MN and TI channels. The reactions with $Br_2^-$ are a byproduct of this work and will not be discussed further, except to say that the measured values with $Ar^+$ and $Kr^+$ are in agreement with the literature data.[9,15] There are several clear trends in the data (see Fig. 4(a)): The reactions of the lighter rare gas cations are faster than those of the heavier rare gas ions, while reactions involving the light halide anions tend to be slower. The rate coefficients across the 12 reactions differ by more than a factor of at least ~60, with some of the reactions so slow that only upper limits could be determined. In contrast, reported rate coefficients for polyatomic-monatomic MN reactions differ by no more than about a factor of 3.[9]

These findings are compatible with accidentally resonant charge transfer in which the attached electron is transferred to excited, nearly resonant states of the rare gas atom. Suitable excited states of the rare-gas atoms are their metastable states and those above because they lie below the Rg ionization limit by approximately the electron affinity of the halogen atoms (~3–3.6 eV). Similar arguments are invoked in the context of thermal-energy reactions of doubly-charged rare-gas ions with rare-gas atoms.[24,25] This suggests that the $Rg^+ + X^-$ reaction rates should be sensitive to the energy difference

$$\Delta E = IE(Rg) - E^*(Rg) - EA(X), \quad (4)$$

where $IE(Rg)$ is the ionization energy of Rg, $E^*(Rg)$ is the energy of the lowest excited state of Rg, and $EA(X)$ is the electron affinity of X. According to Olson,[26] Landau-Zener transitions in MN systems are most effective when the initial and final states intersect at crossing distances $R_x$ from 15 to 50 $a_o$. Because the initial $Rg^+ + X^-$ curve is dominated by the Coulomb potential and is essentially system independent at large distances, $R_x$ may be calculated from only the asymptotic energy difference between the initial and final states, $\Delta E$. In units of $a_o$ for $R_x$ and eV for $\Delta E$, $R_x = 27.2/\Delta E$, meaning that Olson's favorable crossing distances are equivalent to $\Delta E$ = 0.5–1.8 eV. Our experimental data (see Fig. 5) agree with this qualitative expectation: The measured rate coefficients fall off rapidly at crossing radii above 20 $a_o$. Note that the estimated crossing radii refer to the lowest excited $Rg^*$ states; those for the actual dissociating states may be larger.

Hickman[10] derived a simple formula to estimate rate coefficients for MN reactions, and he shows that it works well

TABLE III. Derived total rate coefficients for the indicated $Rg^+ + X^-$ reactions (in $10^{-8}$ $cm^3$ $s^{-1}$ units) with the transfer ionization rate coefficient in parentheses.

| | $X^-$ | | | |
|---|---|---|---|---|
| $Rg^+$ | $Cl^-$ | $Br^-$ | $I^-$ | $Br_2^-$ |
| $Ne^+$ | $3.0 \pm 1.1$[a] | $3.3 \pm 1.2$[a] | $6.5 \pm 1.7$[a] | ... |
| $Ar^+$ | $0.4 \pm 0.2$[b] | $0.5 \pm 0.2$ (0.19) | $2.1 \pm 0.4$ (0.11) | $3.7 \pm 0.8$ |
| $Kr^+$ | <0.2[b] | <0.2[b] | $0.9 \pm 0.2$[a] | $3.2 \pm 0.8$ |
| $Xe^+$ | <0.1[b,c] | <0.3[b] | <0.2[b] | $4.0 \pm 1.5$ |

[a]Transfer ionization is exothermic, but the rate coefficients have not been determined.
[b]Transfer ionization is endothermic.
[c]The rate coefficient for $Xe^+ + Cl^-$ was fixed in the analysis to a value $<10^{-9}$ $cm^3$ $s^{-1}$; see text.

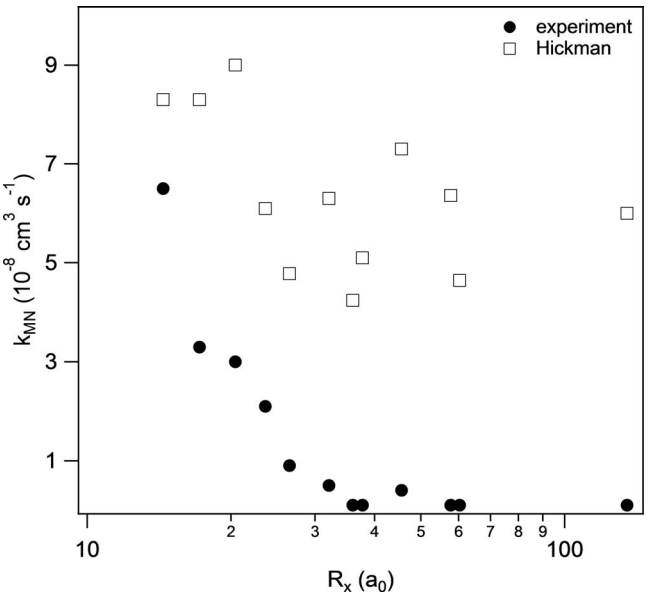


FIG. 5. $Rg^+ + X^-$ rate coefficients from experiment (closed circles) and estimated using Hickman's parameterization, Eq. (5) (open squares) as a function of the crossing radius $R_x$.

in many cases. His formula,

$$k_{MN} = 5.3 \times 10^{-7} \left(\frac{300}{T}\right)^{1/2} \mu^{-1/2} E A^{-0.4} \qquad (5)$$

yielding k (in $cm^3$ $s^{-1}$ units) has the virtue that it depends only on easily available parameters, the temperature T (in Kelvin), the reduced mass $\mu$ of the reactants, and the EA of the halide (in eV). The equation with slightly modified values was found to describe well the variation in MN rate coefficients of polyatomic anions with monatomic cations.[9] However, the derivation assumes that the initial ionic potential curve crosses many final neutral curves and that some of them will occur at favorable crossing radii $R_x$, an assumption that breaks down for some of the reactions here. For instance, the $Xe^+ + Cl^-$ reaction is exothermic by about 8.5 eV, but only a handful of product curves encompassing 3 electronic states of Xe and 2 of Cl are energetically accessible. As may be seen in Fig. 5, the estimating formula comes within a factor of ~2 to the measured values for systems which happen to have a favorable $R_x$ ~20 $a_o$, but seriously overestimates the rate coefficients at larger $R_x$, those that correspond to small $\Delta E$. If one is aware of this limitation, the formula continues to be useful. Indeed the exceptionally strong correlation between rate coefficient and $R_x$ seen in Fig. 5 suggests that crossing radius is the dominant factor contributing to the likelihood of MN. Polyatomic systems are almost assured to have a crossing in the favorable region, resulting in the observed small variability between MN rate coefficients.

A number of MN rate coefficients for reactions of diatomic and polyatomic anions with monatomic cations were previously reported as a function of temperature from 300 to 550 K using the VENDAMS technique.[9] All of the rate coefficients were measured via the difference with either $Ar^+$ or $Kr^+$ with $Cl^-$ or $Br^-$. At the time of that study, those rate coefficients for those reactions were not known, and the data were analyzed under the assumption that the rate coefficients were less than the uncertainty of the experiment of about $2 \times 10^{-9}$ $cm^3$ $s^{-1}$. While this appears to be true in the reactions involving $Kr^+$, the $Ar^+$ reactions occur slightly faster. In light of the current results, the set of MN rate coefficients reported in that study involving $Ar^+$ should be uniformly increased by $4 \times 10^{-9}$ $cm^3$ $s^{-1}$.

It has also been possible to determine product branching ratios between MN and TI for some but not all reactions. For about half of the systems studied, TI is endoergic (Table III); for several other systems background $X^+$ prevented a

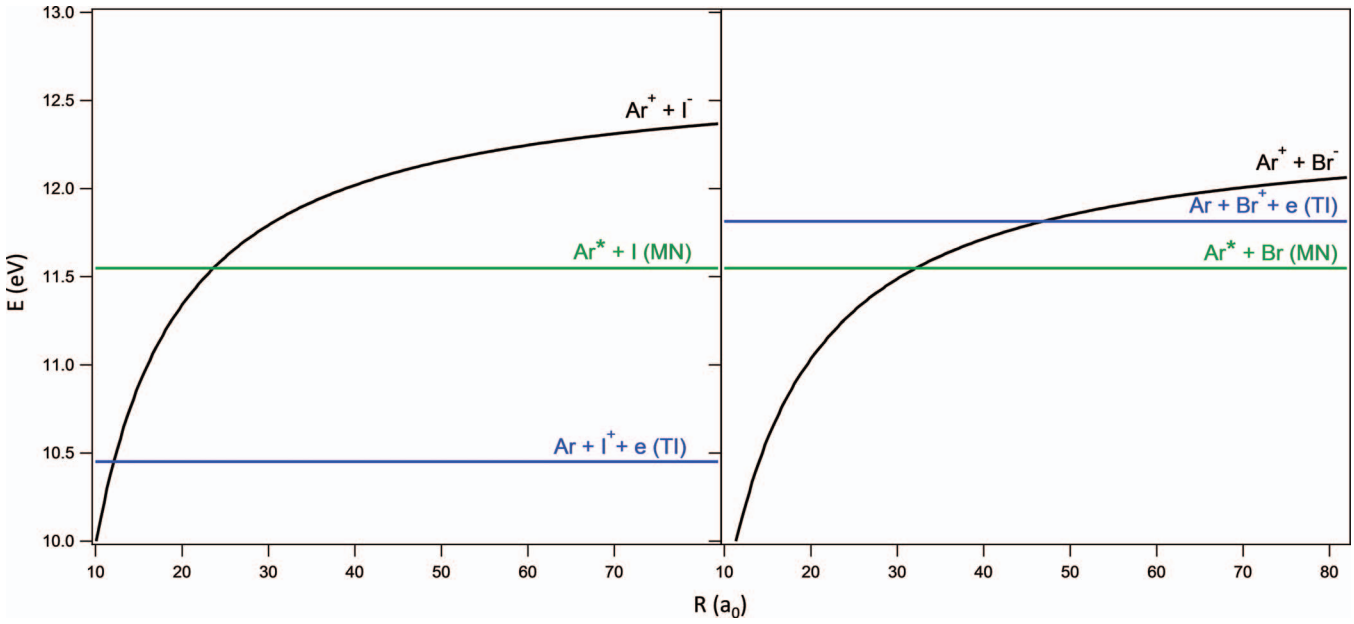


FIG. 6. Schematic of potential energy curves relevant to MN and TI relative to Ar + X for the X = I and X = Br systems. $Ar^*$ refers to the lowest metastable state and the electron energy in the TI final state is taken to be zero.

determination of the TI rate coefficient. A measurable contribution of TI has been found for the reactions of $Ar^+$ with $Br^-$ and $I^-$.[18] While the two TI rate coefficients differ by less than a factor of two, the branching fractions varies much more; TI accounts for ~40% of $Ar^+ + Br^-$, but just ~6% for $Ar^+ + I^-$. Although the dynamics of both TI and MN are unclear, it is worth noting that the smaller TI branching fraction in the latter reaction may be a consequence of the differing energies of the final states.

Figure 6 shows approximate potential energy curves of the relevant ArX (X = Br,I) states relative to the separated Ar and X atoms. The potential curve leading to TI lies ~1.2 eV below that for MN in the $I^-$ reaction, but ~0.6 eV above the MN curve in the Br-reaction. Hence, a colliding $Ar^+$ /$I^-$ pair will first cross the MN curve, while an $Ar^+$/$Br^-$ pair will first cross the TI curve. If one now makes the assumption that the autoionization leading to TI is most efficient when the ejected electron has zero energy (plausible as the inverse process $e + Ar + X^+ \rightarrow Ar^+ + X^-$ is a recombination reaction known to have a maximum cross section at low electron energies), then TI will occur mainly at the crossings between the ionic and TI curves and it would follow that TI is less important in the $I^-$ reaction because the MN reaction reduces the flux reaching the TI crossing.

## CONCLUSION

Mutual neutralization rate coefficients (Table III) have been derived for reactions of rare gas cations ($Ne^+$, $Ar^+$, $Kr^+$, $Xe^{+)}$ with halide anions ($Cl^-$, $Br^-$, $I^-$) for the first time. Unlike MN reactions involving polyatomic species, which vary by no more than a factor of 3, the rate coefficients for the monatomic-monatomic processes vary by at least a factor of 60. Rate coefficients increase down the periodic table ($Cl^-$ to $I^-$) for the halide anions, and up the periodic table ($Xe^+$ to $Ne^+$) for the rare gas cations. Previously reported parameterizations fail to predict the rate coefficients of these reactions, likely due to the breakdown of the assumption that the reactions involve a large density of neutral product states. Instead, the rate coefficients vary strongly according to the exothermicity corrected by the energy of the lowest excited state of the rare gas neutral; systems with such an adjusted exothermicity of around 1 eV, corresponding to a crossing of the neutral and ion potential curves of ~20 $a_o$, show a large rate coefficient comparable to those for MN reactions involving polyatomics. For several of the reactions, competition between mutual neutralization and transfer ionization is observed. For those reactions where it is possible to derive the TI rate coefficient, only the reaction of $Ar^+$ with $Br^-$ has an appreciable fraction of the reaction occurring by that channel.

## ACKNOWLEDGMENTS

A.A.V and N.S.S. are grateful for the support of the Air Force Office of Scientific Research for this work under Project No. AFOSR-2303EP. T.M.M. is under Contract No. FA8718-10-C-0002 from the Institute for Scientific Research of Boston College.

[1]M. R. Flannery, Adv. At. Mol. Opt. Phys. **32**, 117–147 (1994).
[2]D. R. Bates, Adv. At. Mol. Phys. **20**, 1–40 (1985).
[3]W. Schön, S. Krüdener, F. Melchert, K. Rinn, M. Wagner, E. Salzborn, M. Karemera, S. Szücs, M. Terao, D. Fussen, R. Janev, X. Urbain, and F. Brouillard, Phys. Rev. Lett. **59**, 1565–1568 (1987).
[4]M. Stenrup, A. Larson, and N. Elander, Phys. Rev. A **79**, 012713 (2009).
[5]H. S. Lee and R. Johnsen, J. Chem. Phys. **93**, 4868–4873 (1990).
[6]R. E. Olson, J. R. Peterson, and J. Moseley, J. Chem. Phys. **53**, 3391 (1970).
[7]B. L. Whitten, W. L. Morgan, and J. N. Bardsley, J. Chem. Phys. **78**, 1339–1343 (1983).
[8]M. J. Church, and D. Smith, J. Phys. D **11**, 2199–2206 (1978).
[9]T. M. Miller, N. S. Shuman, and A. A. Viggiano, J. Chem. Phys. **136**, 204306 (2012).
[10]A. P. Hickman, J. Chem. Phys. **70**, 4872–4878 (1979).
[11]R. D. Thomas, H. T. Schmidt, G. Andler, M. Bjorkhage, M. Blom, L. Brannholm, E. Backstrom, H. Danared, S. Das, N. Haag, P. Hallden, F. Hellberg, A. I. S. Holm, H. A. B. Johansson, A. Kallberg, G. Kallersjo, M. Larsson, S. Leontein, L. Liljeby, P. Lofgren, B. Malm, S. Mannervik, M. Masuda, D. Misra, A. Orban, A. Paal, P. Reinhed, K. G. Rensfelt, S. Rosen, K. Schmidt, F. Seitz, A. Simonsson, J. Weimer, H. Zettergren, and H. Cederquist, Rev. Sci. Instrum. **82**, 065112 (2011).
[12]N. S. Shuman, T. M. Miller, A. A. Viggiano, and J. Troe, Adv. At. Mol. Opt. Phys. **61**, 209–294 (2012).
[13]N. S. Shuman, T. M. Miller, N. Hazari, E. D. Luzik, and A. A. Viggiano, J. Chem. Phys. **133**, 234304 (2010).
[14]N. S. Shuman, T. M. Miller, R. J. Bemish, and A. A. Viggiano, Phys. Rev. Lett. **106**, 018302 (2011).
[15]N. S. Shuman, T. M. Miller, J. F. Friedman, A. A. Viggiano, S. Maeda, and K. Morokuma, J. Chem. Phys. **135**, 024204 (2011).
[16]R. Johnsen, E. V. Shunko, T. Gougousi, and M. F. Golde, Phys. Rev. E **50**, 3994–4004 (1994).
[17]N. S. Shuman, A. A. Viggiano, and R. Johnsen, J. Chem. Phys. **138**, 204302 (2013).
[18]N. S. Shuman, T. M. Miller, A. A. Viggiano, and R. Johnsen, J. Chem. Phys. **139**, 171102 (2013).
[19]T. M. Miller, A. E. S. Miller, J. F. Paulson, and X. Liu, J. Chem. Phys. **100**, 8841–8848 (1994).
[20]N. S. Shuman, J. F. Friedman, T. M. Miller, and A. A. Viggiano, J. Chem. Phys. **137**, 164306 (2012).
[21]D. Smith, N. G. Adams, and E. Alge, J. Phys. B **17**, 461–472 (1984).
[22]W. C. Lineberger, and L. J. Puckett, Phys. Rev. **186**, 116–127 (1969).
[23]N. S. Shuman, T. M. Miller, C. M. Caples, and A. A. Viggiano, J. Phys. Chem. A **114**, 11100–11108 (2010).
[24]R. Johnsen and M. A. Biondi, Phys. Rev. A **20**, 87–97 (1979).
[25]W. Lindinger, Phys. Scr. **T3**, 115–119 (1983).
[26]R. E. Olson, J. Chem. Phys. **56**, 2979–2984 (1972).

## DISTRIBUTION LIST

DTIC/OCP
8725 John J. Kingman Rd, Suite 0944
Ft Belvoir, VA 22060-6218 1 cy

AFRL/RVIL
Kirtland AFB, NM 87117-5776 2 cys

Official Record Copy
AFRL/RVBXT/Dr. Albert Viggiano 1 cy

This page is intentionally left blank.